Limnol. Oceanogr., 48(3), 2003, 1338–1345

Predicting wave exposure in the rocky intertidal zone: Do bigger waves always lead to larger forces?

Brian Helmuth[1] *and Mark W. Denny*
Stanford University, Hopkins Marine Station, Pacific Grove, California 93950

Abstract

Hydrodynamic forces from breaking waves are among the most important sources of mortality in the rocky intertidal zone. Information about the forces imposed by breaking waves is therefore critical if we are to interpret the mechanical design and physiological performance of wave-swept organisms in an ecologically and evolutionarily relevant context. Wave theory and engineering experiments predict that the process of wave breaking sets a limit on the maximum force to which organisms can be subjected. Unfortunately, the magnitude of this limit has not been determined on rocky shores. To this end, at a moderately exposed shore in central California, we measured the maximum hydrodynamic forces imposed on organism-sized benthic objects and related these forces to nearshore significant wave heights. At 146 of 221 microsites, there was a significant and substantial positive correlation between force and wave height, and at 130 of these microsites, force increased nonlinearly toward a statistically defined limit. The magnitude of this limit varied among sites, from 19 to 730 newtons (N). At 37 other sites, there was no significant correlation between surf zone force and wave height, indicating that increased wave height did not translate into increased force at these sites either. At only 16 sites did force increase in proportion to wave height without an apparent upper bound. These results suggest that for most microsites there is indeed a limiting wave height beyond which force is independent of wave height. The magnitude of the limit varies substantially among microsites, and an index of local topography was found to predict little of this variation. Thus, caution must be exercised in any attempt to relate observed variations in ocean ''waviness'' to the corresponding rates of microsite disturbance in intertidal communities.

Rocky intertidal invertebrates and algae live in a world of extreme environmental severity, and the risk of damage or dislodgment from wave-generated forces is thought to be among the most important determinants of survival in this habitat (e.g., Dayton 1971; Levin and Paine 1974; Koehl 1979; Paine 1979; Paine and Levin 1981; Sousa 1984; Denny 1987, 1988; Carrington 1990, 2002; Bertness et al. 1991; Hunt and Scheibling 1996; Blanchette 1997). Quantifying the hydrodynamic forces acting on organisms, and how they vary in space and in time, is therefore key to understanding the evolutionary and ecological consequences of morphological design and the subsequent effects of wave-driven forces on the dynamics of intertidal ecosystems (Denny 1988; Koehl 1996; Denny and Wethey 2001; Carrington 2002).

The use of engineering theory to study these issues has proven fruitful and has led to a deeper understanding of how intertidal organisms are able to withstand the rigors of wave-exposed shores (e.g., Koehl 1979; Denny 1988; Carrington 1990, 2002; Bell and Gosline 1996; Denny et al. 1998; Gaylord 2000). Understanding how organisms resist damage and dislodgment, however, also requires an estimate of the hydrodynamic forces experienced by organisms in the field (Denny 1995), and recent evidence has revealed how complex it can be to predict forces at spatial scales relevant to organisms (Gaylord 1999, 2000).

Engineers have long been interested in the forces that waves can exert, but their measurements have focused on the pressures imposed as water strikes a breakwater or cylindrical support member (e.g., Chan et al. 1995; Kobayashi and Demerbilek 1995; Bird et al. 1998; Kobayashi 1999; Bullock et al. 2001). The pressure field can be used to predict the load on the entire structure (the parameter of primary importance to engineers) but is of little practical utility for predicting the lift and drag forces that act on individual organisms.

Direct records of wave-induced forces have been obtained at the scale of individual organisms (e.g., Jones and Demetropoulos 1968; Koehl 1977; Bell and Denny 1994; Denny 1995; Gaylord 1999, 2000), but these measurements are difficult to conduct in this severe environment. An attractive alternative approach is to generate predictions of forces from measurements of nearshore wave height (Denny 1995; Carrington 2002). This latter approach is of particular interest because wave height measurements are readily available from buoys (e.g., those maintained by the U.S. National Data Buoy Center) and provide a potential means of comparing widely spaced sites and of estimating forces over long periods of time. Usually, these data are reported using an index of ocean ''waviness,'' with H_s the significant wave height. H_s is the average of the highest ⅓ of wave heights recorded during any particular interval (*see* Denny [1988, 1995] for an explanation of significant wave height).

It has generally been assumed by intertidal ecologists that the higher the waves are (i.e., the larger H_s is), the larger the forces imposed on intertidal organisms. Carstens (1968) and Denny (1988, 1995) have pointed out, however, that both

[1] To whom correspondence should be addressed. Present address: University of South Carolina, Department of Biological Sciences and Marine Sciences Program, Columbia, South Carolina 29208 (helmuth@biol.sc.edu).

Acknowledgments
This research was supported by NSF grants OCE 9633329 and 9985946 to M.W.D. Helpful comments on the manuscript were provided by Chris Harley.

wave theory and engineering measurements predict that wave-breaking sets an upper limit to this relationship. As waves move into shallow water they become steeper (their wavelength decreases and their height increases) and they eventually become unstable. The timing of this instability depends on a variety of factors (wave period and beach slope are prominent). On shores with a gentle slope, waves typically break when their height is approximately half the water's depth (Thornton and Guza 1983). On the steep slopes typical of rocky shores, waves generally break when their height is approximately equal to the local water depth (Galvin 1972). In either case, the higher the wave, the farther offshore it breaks. Because exceptionally high waves typically break far from the shore, they are likely to have lost much of their energy to turbulent dissipation by the time they can interact with plants and animals in the intertidal zone (Thornton and Guza 1983). In this fashion, wave breaking can set a limit to the ''wave exposure'' of intertidal sites.

Although there can be little doubt that for each point on the shore a limit exists to the wave-induced force that can be imposed, the extreme complexity of water motion in breaking waves currently precludes the prediction of an accurate, site-specific limit to wave force. Indeed, this limit is likely to be very sensitive to the local topography of the shore and, therefore, could vary substantially from one point to the next. Our current inability to predict maximum wave forces solely from fluid dynamic principles, and the likely variation among sites, hampers our understanding of intertidal ecology.

Here, we describe a set of measurements in which we relate maximum onshore forces (measured at a spatial scale relevant to individual intertidal organisms) to maximum significant wave height. We show that for most of the locations at which measurements were conducted, there is indeed a statistically definable upper limit to wave-induced force and that increasing wave height does not always lead to increased onshore forces. The implications of this limit are discussed.

Materials and methods

Measurements of organismally relevant forces were collected at 221 microsites on the shore adjacent to the Hopkins Marine Station in Pacific Grove, California (36°36′N, 121°53′W), from October 1997 to May 1999. The term ''microsite'' is used here to differentiate the spatial scale of our individual measurements (each of which encompasses a circular area approximately 10 cm in diameter) from that of a ''site,'' which in much intertidal work refers to an area measured in square meters to hundreds of square meters. The majority of these microsites (175) were arrayed on a 200-m-long horizontal transect situated 1.5 m above mean lower low water (MLLW) in the midintertidal mussel zone. The remaining microsites were on vertical walls in the high intertidal zone. Site- and time-specific maximum forces, F, were recorded using dynamometers based on the design of Bell and Denny (1994) and described in Denny and Wethey (2001). Briefly, the device records the maximum hydrodynamic force imposed on a roughened sphere (typically a Wiffle golf ball of diameter 40.8 mm), which is connected to a spring via a string equipped with a slider. The spring, string, and slider are housed in a plastic sleeve, which is inserted into a hole drilled into the substratum and secured with a threaded neck. Each dynamometer was deployed for periods of 1 d to 2 weeks (usually 1–5 d), recording the maximum force imposed on the ball during that interval.

The distance over which the slider moved was calibrated using a series of weights, so that distance moved could be translated into maximum force (measured in newtons). Because dynamometers at the most exposed microsites were frequently subjected to forces at or near the maximum force the instrument was capable of recording, the standard wiffle golf balls at these sites were replaced with smaller (diameter = 25.4 mm) polypropylene balls that were roughened by machining grooves into their surfaces. The drag force recorded by these smaller spheres was then extrapolated to that which would have been recorded for the larger balls by multiplying by the ratio of projected areas for the two spheres. Measurements in a wind tunnel at Reynolds numbers equivalent to those in the surf zone (6×10^4 to 2×10^5) showed that at over a range of velocities, the average ratio of drag forces between small and large balls (2.66 with a 95% confidence limit of 0.28) was not significantly different from the actual ratio of projected areas (2.61). Smooth spheres in laminar flow are subject to an abrupt decrease in drag coefficient in the Reynolds number range 10^4–10^5 (Sarpkaya and Isaacson 1981; Vogel 1994). However, because of their rough surface and the turbulence they encounter in the benthic boundary layer, no such reduction in drag coefficient is expected for the balls used here (Sarpkaya and Isaacson 1981), and none was observed.

Concurrently, a pressure transducer (Sea-Bird 26-03 Seagauge) was deployed in 10 m of water at a benthic site ~50 m offshore of the intertidal measurements. The wave gauge recorded the significant nearshore wave height over a period of ~9 min, every 6 h. The maximum significant wave height for the period during which each dynamometer was deployed was then calculated from the wave height data. To avoid errors in the use of linear wave theory to correct for pressure attenuation, the high-frequency cutoff for the calculation of H_s was set at 0.318 Hz, approximately three times the typical peak frequency of 0.11 Hz. In general, at this site, there is very little wave energy at frequencies near 0.3 Hz, so any errors from transformation should be minor.

At least 20 measurements of maximum force, F, were collected for each microsite (mean = 38, SD = 15). At each microsite, forces were analyzed as a function of the maximum significant wave height recorded during the deployment period. This analysis allowed us to divide the microsites into four categories.

Category 1 (nonlinear, bounded)—At these microsites, there was a significant ($p \leq 0.05$) and substantial ($r^2 \geq 0.25$) correlation between force and wave height, and the data were fit by a model that incorporated an asymptote, supposing that

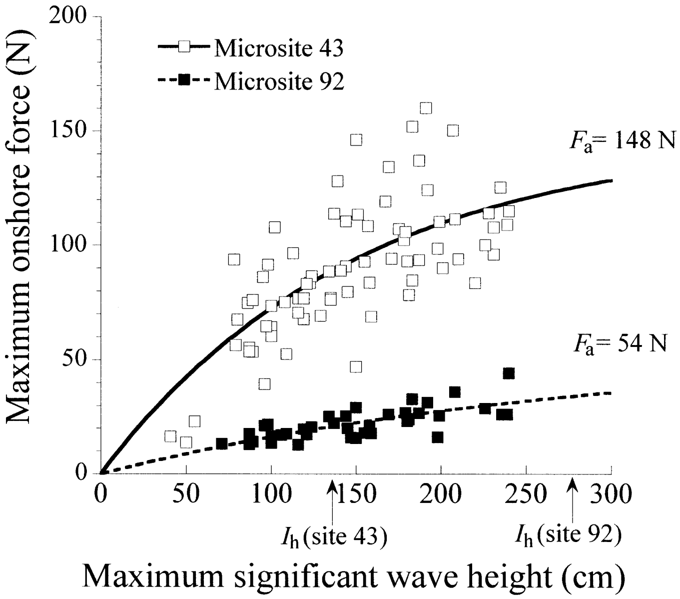

Fig. 1. Relationship between onshore force (N) measured at the level of intertidal organism as a function of nearshore maximum significant wave height (H_s, cm) for two microsites. For the two examples shown, forces increase asymptotically with significant wave height. At microsite 43, forces level off at wave heights above ~140 cm to a maximum force of 148 N. At a nearby site (microsite 92), forces increase much more slowly with wave height, and only achieve a maximum of ~54 N, leveling off for wave heights greater than ~275 cm.

above some wave height force no longer increased with increasing wave height.

$$\hat{F} = F_a\left(1 - \exp\left[\frac{-H_s}{I_h}\right]\right) \quad (1)$$

This model is based on an equation often used by plant physiologists to relate photosynthesis to irradiance. In our case (as in theirs), an upper limit to a process is known to exist; the task at hand is to define that limit. Here $\hat{F}$ is the force predicted to be recorded by a dynamometer (in newtons, scaled to a 40.8-mm-diameter sphere), F_a is the asymptotic force, and H_s is, again, the maximum significant wave height (cm, Fig. 1). I_h is the wave height at which maximum onshore forces is within 37% (= $1/e$) of F_a (Fig. 1).

We conducted an additional test to confirm that a definable limit to wave force does indeed exist at Category 1 sites. First, we normalized the individual forces recorded at each point on the rock, F, to the predicted asymptotic force at that site, F_a.

$$F_n = \frac{F}{F_a} \quad (2)$$

The significant wave height corresponding to each F was normalized to I_h at that site.

$$H_n = \frac{H_s}{I_h} \quad (3)$$

If our hypothesis is correct, at high H_n, normalized wave force will be independent of normalized wave height, whereas at low H_n, F_n will increase with increasing H_n. To test for this behavior, the normalized data pairs (F_n, H_n) were divided into two categories: those for which the normalized wave heights were ≥ 2.5 (those within ~10% of the asymptote) and those for which the normalized wave heights were <2.5. A test for correlation was then conducted on each category. The choice of $H_n = 2.5$ as the dividing line between "low" and "high" is based on visual examination of the data. Any value of $H_n \geq 2.5$ could be used without affecting this result.

Category 2 (linear, unbounded)—For these microsites, there was again a significant correlation between force and wave height, but the data were better modeled by a regression that supposed that force at the substratum increased linearly with increasing wave height and that the y-intercept was equal to zero. Microsites were included in this category if the r^2 of the linear model was greater than the r^2 for the nonlinear model described above for Category 1.

Category 3—At these microsites there was no significant correlation between force and nearshore wave height ($p > 0.05$). We interpret this lack of statistical dependence as an indication that, for the purposes of prediction, forces were effectively independent of wave height for the range of wave heights encountered in this study. In other words, we suppose that even at the lowest wave height encountered in this study, these microsites are already at their limit. Force at each of these microsites was characterized by the average value.

Category 4—At these microsites there was a significant ($p \leq 0.05$) but not substantial ($r^2 < 0.25$) correlation between force and wave height. In these cases, we do not feel comfortable drawing conclusions about the relationship of intertidal forces to the wave height offshore, and these data were removed from further consideration.

The F–H_s relationships of Categories 1–3 were used to generate predictions of maximum forces at each relevant microsite for a series of fixed significant wave heights spanning the range of wave heights recorded at Hopkins Marine Station (H_s = 50–350 cm). These predictions were then used to explore the potential correlation between topography and the force experienced at each microsite.

The local topography of the substratum was measured at each of the microsites. The objective of these measurements was to create an index of the topographical potential for a given location to be exposed to wave-induced hydrodynamic forces. Experience led us to believe that this index should include (1) the azimuth of the location relative to the direction of wave approach, (2) the slope of the substratum at the location, and (3) the presence or absence of offshore obstacles in the path of wave approach. A location facing directly into oncoming waves with a vertical slope and no offshore obstacles has the greatest potential to encounter large forces, whereas locations with lesser slopes facing obliquely to the waves and sheltered by obstructions have less potential. We propose that the following index appropriately quantifies these ideas:

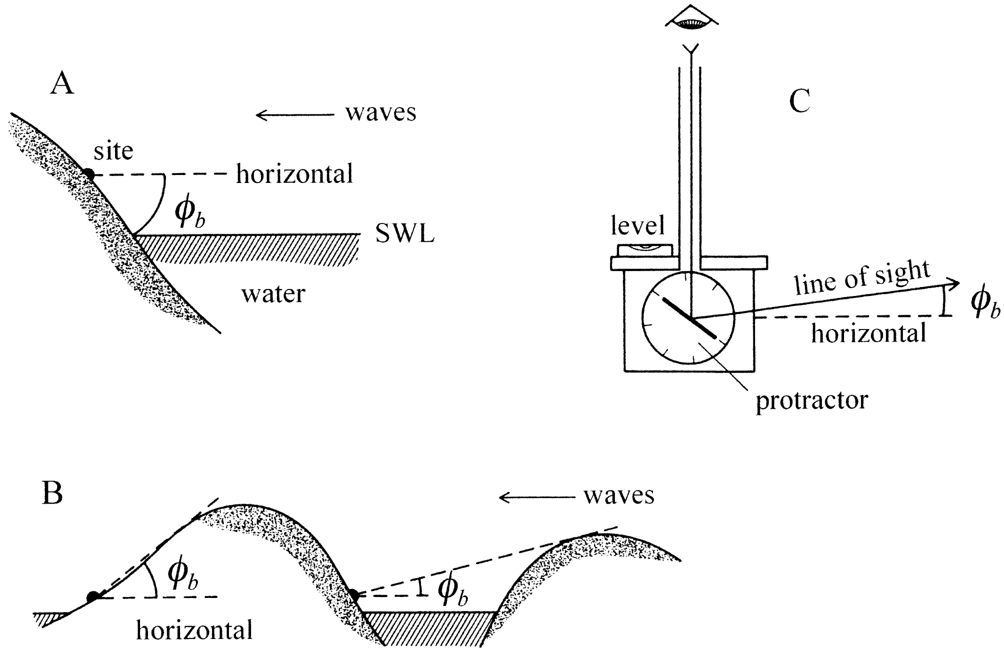

Fig. 2. Definitions related to the measurement of the blocking angle, ϕ_b. The angle is measured in a vertical plane passing through the site along the direction of wave approach and is taken relative to the top of the nearest obstruction, as shown in examples A and B. Sightings are conducted using the apparatus shown in example C. One sights down the vertical tube with the plane of the protractor aligned with the prevailing direction of incoming waves. The vertical angle of this line of sight is then adjusted by rotating a mirror attached to the protractor so that the image of the top of the nearest obstacle (or the intersection of the water with the shore) is centered. The angle of the mirror then provides a measure of ϕ_b. Note that a change of 2° in the blocking angle results in a change of only 1° in the angle of the protractor.

$$T = \frac{[\cos(\theta_w - \theta_s) \times \sin \phi_s] - c \sin \phi_b + 1 + c}{2 + 2c} \quad (4)$$

Here θ_w is the compass direction from which waves approach the shore and θ_s is the compass angle of the horizontal component of the location normal. Thus, $\theta_w - \theta_s$ is a measure of how obliquely the waves strike the site. ϕ_s is the slope of the shore at the location, and ϕ_b is the ''blocking'' angle, as shown in Fig. 2. Blocking angle is measured by sighting along the line of wave approach and noting the angle to the top of the nearest obstruction. In the absence of obstructions, ϕ_b is measured to the point where the water reaches the shore at mean lower low water. Thus, ϕ_b varies from $+90°$ for a site on a vertical wall facing away from the waves to $-90°$ for a site on a vertical wall facing into the waves.

The index T varies between 0 and 1. As proposed, it is highest for vertical locations ($\phi_s = 90°$) that face the oncoming waves ($\theta_w = \theta_s$) without obstacles ($\phi_b = -90°$) and is lowest for vertical locations on the down-wave sides of obstacles.

The horizontal orientation of each location was measured as follows. A plastic rectangle (15 × 8 cm) was held with its flat face horizontal and its short edge held firmly against the rock surface. A magnetic compass was then held against the long face of the rectangle to measure the compass angle of the horizontal component of the location normal (θ_s). The vertical component of the vector normal to the substratum at that location (ϕ_s, the local slope of the shore) was measured using an electronic inclinometer (Wedge Innovations) with a length of 15 cm. The blocking angle was measured using the apparatus shown in Fig. 2C.

The value of c in Eq. 4 (which weights the contribution of offshore obstacles to the index) is chosen to provide the greatest correlation between T and the maximum wave force. A value of c = 0.4 was used here.

Results

Predicting onshore forces from nearshore waves—Of the 221 microsites, 184 (83%) showed a significant, positive correlation with wave height (Categories 1, 2, and 4). At the remaining 37 microsites (17%), intertidal force was not statistically dependent on wave height (Category 3).

Of the 184 microsites where inshore force was demonstrably dependent on wave height, 146 (80%) showed a relationship that was deemed to be substantial ($r^2 \geq 0.25$, Categories 1 and 2). At 16 of these 146 microsites (11%), wave force appeared to increase linearly with increasing wave height, without apparent limit (Category 2). However, at the vast majority of these 146 microsites ($n = 130$, 89%), force appeared to have a definable limit, presumably set by wave breaking (Category 1). The asymptotic maximum force for

Table 1. Summary statistics for division of microsites into four categories.

	Mean	SD	Min	Max
Category 1 (nonlinear, n = 130)				
Sample size per site	40	15	20	80
Topography index (T)	0.64	0.21	0.08	0.94
F_a	105.10	105.90	19.10	730.00
I_h	0.45	0.24	0.19	1.50
r^2	0.41	0.10	0.25	0.66
Relative error (%)	22.13	5.06	11.01	44.86
Absolute error (N)	9.09	5.32	1.71	30.79
Category 2 (linear, n = 16)				
Sample size per site	41	14	31	70
Topography index (T)	0.72	0.08	0.55	0.84
Slope	0.39	0.13	0.20	0.55
r^2	0.54	0.15	0.35	0.81
Relative error (%)	30.61	4.73	23.75	39.59
Absolute error (N)	15.83	5.00	8.97	23.79
Category 3 (Poor fit,* no significant regression,** n = 37)				
Sample size per site	32	6	21	48
Topography index (T)	0.48	0.25	0.12	0.84
Category 4 (Poor fit,* significant regression,** n = 38)				
Sample size per site	36	10	22	59
Topography index	0.53	0.23	0.14	0.85

* $r^2 < 0.25$.
** Regression of measured force (F) versus maximum significant wave height (H_s).

the Category 1 microsites varied from 19 to 730 N, with a mean of 105 N (Table 1). Values of r^2 for these regressions ranged from 0.26 to 0.81, with a mean (±1 SD) of 0.43 ± 0.11. The corresponding probability values of the curve fits ranged from effectively 0 to a maximum of 0.01, with a mean of 0.0007 ± 0.0020.

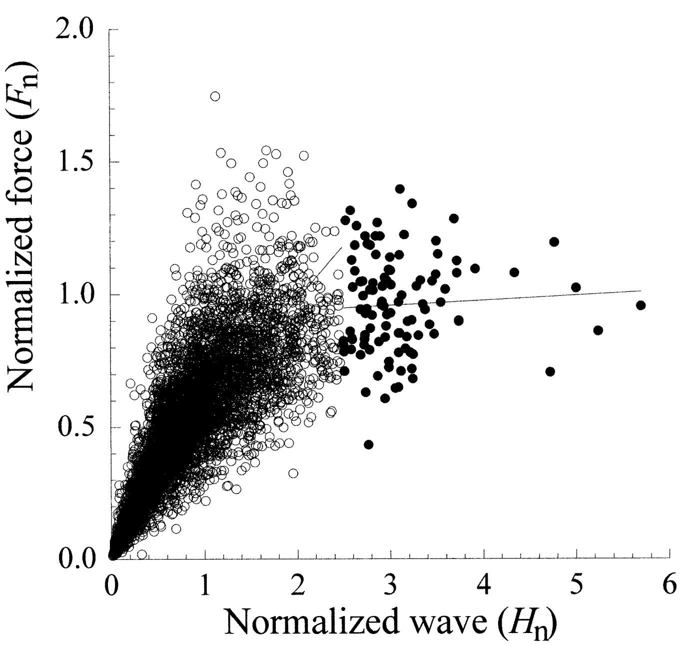

Fig. 3. Data from all sites determined to display a ''Category 1'' (asymptotic) curve fit, normalized to F_a and I_h for each microsite. Below a normalized wave height (H_n) of 2.5 (open circles) there is a significant, positive correlation between normalized force, F_n, and normalized wave height, H_n. Data above H_n = 2.5 show no significant correlation.

Average values of wave forces at Category 3 sites ranged from 15 to 165 N, with a mean of 32.3 ± 29.2 N. The coefficient of variation (SD/mean) for data collected at Category 3 microsites was fairly small (0.28 ± 0.06), confirming that the averages of the data collected at these locations were representative of an actual limit to wave forces. For comparison, we also calculated the predicted F_a for these sites (with Eq. 1). These predicted asymptotic forces differed from the average values by only ~9%, confirming that forces at these microsites achieved a maximum, asymptotic value even at low wave heights. Note that the lack of correlation between F and H_s at the Category 3 sites was not due to any constriction of the range of wave heights at which these force measurements were conducted. Forces were measured at these sites over the same range of wave heights as for other sites.

Category 4 microsites (the locations for which there was a significant, but not substantial, correlation with wave height, n = 38) formed only 17% of all microsites. Significance values of the curve fits ranged from 0.001 to 0.04, with a mean level of significance of 0.018 ± 0.011.

Analysis of normalized Category 1 data confirmed a definable asymptote to maximum force (Fig. 3). At scaled wave heights <2.5, normalized forces showed a significant correlation with wave height (n = 5,056; $F_{1, 5,055} = 8,483$; $p < 0.0001$, $r^2 = 0.63$). At scaled wave heights ≥2.5, there was no significant correlation between scaled force and scaled wave height (n = 105; $F_{1,104} = 0.34$; $p > 0.05$, $r^2 = 0.003$).

Accuracy of force predictions—Relative error: At the 146 Category 1 and 2 locations, relative error, defined as

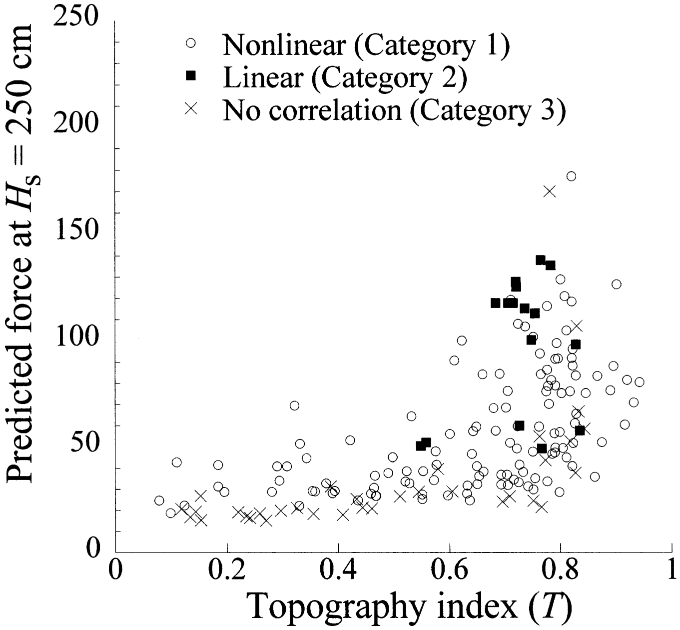

Fig. 4. Effect of topography index, T, on predicted maximum force. The data shown are the predicted force (based on curve fits) at a maximum significant wave height (H_s) of 250 cm. Predicted force appears to increase exponentially with T, and a regression of log (force) versus T at a range of maximum significant wave heights shows a significant relationship (*see Table 2*).

$$\text{relative error} = 100\frac{|F - \hat{F}|}{F} \quad (5)$$

was typically not significantly correlated with wave height (123 microsites, $p > 0.05$), although at a few microsites, relative error decreased significantly ($p \leq 0.05$) with increasing wave height (Category 1 microsites: mean slope = −0.136, $n = 15$; Category 2 microsites: mean slope = −0.174, $n = 8$; wave height for the regressions is in centimeters, relative error is percent).

Absolute error: Mean absolute error was slightly higher at sites with linear fits (Category 2) than at sites with nonlinear fits (Category 1) (Table 1). Absolute error

$$\text{absolute error} = |F - \hat{F}| \quad (6)$$

was typically statistically independent of wave height ($n = 105$), although at a few microsites absolute error increased significantly with increasing wave height (Category 1: mean slope = 0.057, $n = 34$; Category 2: mean slope = 0.093, $n = 7$; wave height for the regression is in centimeters, absolute error is in newtons).

The ability of our models to predict relative error either remained constant across wave heights or increased with wave height, whereas our ability to predict absolute wave forces either remained constant or decreased with wave height. Both relative and absolute errors were higher for Category 2 microsites (where force was linearly related to wave height), as compared to Category 1 microsites (where force was asymptotic) (Table 1).

Table 2. Statistical results for regressions of log(F) versus T over a range of H_s (cm). $n = 146$.*

H_s	Intercept	Slope	r^2	$F_{1,145}$ value
50	0.98	0.45	0.21	38.0
100	1.15	0.52	0.28	54.0
150	1.23	0.59	0.32	66.0
200	1.27	0.65	0.34	73.0
250	1.29	0.69	0.35	76.1
300	1.30	0.73	0.35	76.6
350	1.30	0.77	0.35	75.7

* Only Category 1 and 2 sites are included. All regressions, $p \leq 0.0001$.

Effect of microsite topography on wave exposure—For a given significant wave height (H_s), there was a positive trend between the maximum force predicted at a microsite ($\hat{F}$) and the topographic index (T) of that site (Categories 1 and 2 only). This relationship appeared to be approximately exponential (Fig. 4), and regressions of log(F) vs. T showed a significant, positive relationship at all values of H_s considered (Table 2). Likewise, at Category 1 microsites, there was a significant exponential relationship between the asymptotic force, F_a, predicted for that site and T (regression of log[F_a] vs. T: $F_{1,129} = 50.3$, $r^2 = 0.29$, $p \leq 0.0001$, $n = 130$). Similarly, there was a significant (although not substantial) exponential relationship between I_h and T at these sites (log[I_h] vs. T: $F_{1,129} = 14.6$, $r^2 = 0.11$, $p \leq 0.0002$, $n = 130$).

At any given wave height, there was considerable variation in the predicted force among our 221 microsites (Table 3). Within the 200-m stretch of shore used in these measurements (a length of shoreline that ecologists might consider to be a single, moderately exposed site), the force imposed on the most "exposed" microsite was between 11.4 and 19.7 times that imposed on the most "protected" microsite, depending on wave height.

Discussion

The rocky intertidal zone has long served as an effective testing ground for examining the interactive effects of biotic and abiotic variables on community structure (Connell 1961; Paine 1966; Dayton 1971; Menge 1976; Paine and Levin 1981; Wethey 1985; Dial and Roughgarden 1998; Carrington 2002). In particular, physical disturbance resulting from wave-generated forces has been shown to be a key ecological feature of exposed shorelines—it opens up space, thereby permitting the settlement of competitively subordinate

Table 3. Predicted forces over a range of H_s (cm) for Category 1–3 sites.

H_s	Max	Min	Average	SD/Mean	Max/Min
50	165.3	8.4	21.9	0.75	19.7
100	165.3	14.5	33.6	0.60	11.4
150	165.3	14.6	42.9	0.59	11.4
200	194.2	14.6	50.4	0.61	13.3
250	220.2	14.6	56.7	0.63	15.1
300	240.8	14.6	62.1	0.66	16.5
350	257.0	14.6	66.8	0.69	17.7

primary space occupiers (Levin and Paine 1974; Paine and Levin 1981; Dial and Roughgarden 1998) and alters the strength of interspecific interactions (e.g., Menge 1976). Understanding the morphological, behavioral, and structural adaptations that allow intertidal organisms to function and persist in such a physically challenging environment therefore has become the focus of many recent studies. This exploration has been accelerated through the use of biomechanical theory, which permits a rigorous, mechanistic, and quantitative means of exploring how such factors as organism shape, size, and material properties affect the risk of dislodgment and mechanical failure (e.g., Koehl 1979, 1996; Denny et al. 1985; Denny 1988; Carrington 1990, 2002; Bell and Gosline 1996; Denny and Gaylord 1996; Blanchette 1997; Denny et al. 1998). In order to place these studies into an ecologically relevant context, however, we need a better understanding of what forces are in the field, and how they change over a range of spatial and temporal scales (Gaylord 1999, 2000).

Global change—The task of quantitatively predicting hydrodynamic forces takes on a particular relevance in light of data showing that large areas of the world's oceans have become ''wavier'' in recent years (Goldenberg et al. 2001), and that El Niño-Southern Oscillation (ENSO) events (which often are accompanied by unusually large waves) have increased in both frequency and intensity (Bacon and Carter 1991; Trenberth 1993; Wellington and Dunbar 1995). In this regard long-term records of nearshore significant wave height could serve as a potentially invaluable resource for examining temporal trends in the effects of wave climate on the exposure on intertidal communities. But this utility of long-term wave records can be realized only if we can accurately predict intertidal forces from these wave heights. The results of this study suggest that these predictions must be made with caution.

First, our measurements clearly show that at most microsites (130 of 221, Category 1) intertidal forces under extreme wave conditions cannot be predicted accurately by a linear extrapolation from less severe conditions. Instead, there appears to be a microsite-specific maximum force, presumably set by wave breaking. At the additional 37 Category 3 sites, force is apparently independent of wave height for all wave heights encountered in this study, again a result that likely is due to the tendency of waves to break and dissipate before reaching these microsites. Because of this behavior, most of our 221 microsites showed virtually no increase in force with significant wave height for $H_s > \sim 2$–2.5 m. In light of the fact that the average significant wave height at open-coast sites in Washington, Oregon, and California is already 2–2.5 m (Denny 1995), if our results are at all typical, they suggest that any increase in waviness might have little effect on the majority of intertidal microsites on the west coast of North America.

In contrast, at the minority of microsites where the asymptotic force does not occur until a much larger significant wave height (e.g., our Category 2 microsites), forces (and, presumably, rates of mortality) could indeed increase as waviness increases. Given this disparity in behavior among microsites, increasing significant wave height from climate change is likely to lead to an increase in spatial heterogeneity in a wave-generated disturbance. For example, for $H_s > 50$ cm, an increase in wave height leads to both an increase in the range of wave-induced forces and a general increase in the coefficient of variation (SD/mean) among the microsites we examined (Table 3).

Measuring exposure of microsites—Our measurements demonstrate that local topography can indeed play an important role in determining the potential ''exposure'' of a microsite (Fig. 4) but that our topographic index, T, can explain only 21–35% of the overall variation in force (r^2, Table 2). This suggests that although high-T sites are in general more likely to experience higher rates of wave disturbance than are low-T sites, it could be exceedingly difficult for an intertidal ecologist using this type of index to determine a priori precisely which microsites are ''exposed'' and which are ''protected.'' To obtain improved predictability, one must take into account the topography of the shore along the entire path of a wave leading up to the microsite, and quantifying this topography using current technology is prohibitively labor intensive.

Furthermore, the heterogeneity among microsites (noted above) makes it difficult even to classify a site as to its exposure. Is it the mean force among microsites, the maximum force among microsites, or the range of forces among microsites that best characterizes a site? The answer to this question is likely to involve substantial further experimentation. Unfortunately, the results of this study demonstrate that quantifying onshore forces at scales relevant to organisms can be complex and time consuming. Clearly, knowledge of offshore wave heights and a simple index of nearshore topography can provide only a rough prediction of the force that will be imposed at a given spot on the shore. As a consequence, if we want to know intertidal forces, there is currently no substitute for measuring these forces directly at the microsites of interest (e.g., an experimental plot or transect).

Our results suggest that a limit to inshore force indeed exists, that it varies substantially among microsites, and that caution therefore must be exercised in any attempt to relate observed increases in ocean waviness to the corresponding rates of disturbance in intertidal communities.

References

Bacon, S., and D. J. T. Carter. 1991. Wave climate changes in the North Atlantic and North Sea. Int. J. Clim. **11:** 545–558.

Bell, E. C., and M. W. Denny. 1994. Quantifying ''wave exposure'': a simple device for recording maximum velocity and results of its use at several field sites. J. Exp. Mar. Biol. Ecol. **181:** 9–29.

———, and J. M. Gosline. 1996. Mechanical design of mussel byssus: Material yield enhances attachment strength. J. Exp. Biol. **199:** 1005–1017.

Bertness, M. D., S. D. Gaines, D. Bermudez, and E. Sanford. 1991. Extreme spatial variation in the growth and reproductive output of the acorn barnacle *Semibalanus balanoides.* Mar. Ecol. Prog. Ser. **75:** 91–100.

Bird, P. A. D., A. R. Crawford, P. J. Hewson, and G. N. Bullock. 1998. An instrument for field measurement of wave impact pressures and seawater aeration. Coastal Eng. **35:** 103–122.

BLANCHETTE, C. A. 1997. Size and survival of intertidal plants in response to wave action: A case study with *Fucus gardneri.* Ecology **78:** 1563–1578.

BULLOCK, G. N., A. R. CRAWFORD, P. J. HEWSON, M. J. A. WALKDEN, AND P. A. BIRD. 2001. The influence of air and scale on wave impact pressures. Coast. Eng. **42:** 291–312.

CARRINGTON, E. 1990. Drag and dislodgment of an intertidal macroalga: Consequences of morphological variation in *Mastocarpus papillatus* Kutzing. J. Exp. Mar. Biol. Ecol. **139:** 185–200.

———. 2002. Seasonal variation in the attachment strength of blue mussels: Causes and consequences. Limnol. Oceanogr. **47:** 1723–1733.

CARSTENS, T. 1968. Wave forces on boundaries and submerged bodies. Sarsia **34:** 37–60.

CHAN, E.-S., H.-F. CHEONG, AND B. C. TAN. 1995. Laboratory study of plunging wave impacts of vertical cylinders. Coastal Engineering **25:** 87–107.

CONNELL, J. H. 1961. The influence of interspecific competition and other factors on the distribution of the barnacle *Chthamalus stellatus.* Ecology **42:** 710–723.

DAYTON, P. K. 1971. Competition, disturbance, and community organization: The provision and subsequent utilization of space in a rocky intertidal community. Ecol. Monogr. **41:** 351–389.

DENNY, M. W. 1987. Lift as a mechanism of patch initiation in mussel beds. J. Exp. Mar. Biol. Ecol. **113:** 231–245.

———. 1988. Biology and the mechanics of the wave-swept environment. Princeton Univ. Press.

———. 1995. Predicting physical disturbance: Mechanistic approaches to the study of survivorship on wave-swept shores. Ecol. Monogr. **65:** 371–418.

———, AND B. GAYLORD. 1996. Why the urchin lost its spines: Hydrodynamic forces and survivorship in three echinoids. J. Exp. Biol. **199:** 717–729.

———, AND D. S. WETHEY. 2001. Physical processes that generate patterns in marine communities, p. 3–37. *In* M. E. Hay [ed.], Marine community ecology. Sinauer.

———, T. L. DANIEL, AND M. A. R. KOEHL. 1985. Mechanical limits to size in wave-swept organisms. Ecol. Monogr. **55:** 69–102.

———, B. GAYLORD, B. HELMUTH, AND T. DANIEL. 1998. The menace of momentum: Dynamic forces on flexible organisms. Limnol. Oceanogr. **43:** 955–968.

DIAL, R., AND J. ROUGHGARDEN. 1998. Theory of marine communities: The intermediate disturbance hypothesis. Ecology **79:** 1412–1424.

GALVIN, C. 1972. Waves breaking in shallow water, p. 413–455. *In* R. Meyer [ed.], Waves on beaches and the resulting sediment transport. Academic Press.

GAYLORD, B. 1999. Detailing agents of physical disturbance: Wave-induced velocities and acceleration on a rocky shore. J. Exp. Mar. Biol. Ecol. **239:** 85–124.

———. 2000. Biological implications of surf-zone flow complexity. **45:** 174–188.

GOLDENBERG, S. B., C. W. LANDSEA, A. M. MESTAS-NUÑEZ, AND W. M. GRAY. 2001. The recent increase in Atlantic hurricane activity: Causes and implications. Science **293:** 474–479.

HUNT, H. L., AND R. E. SCHEIBLING. 1996. Physical and biological factors influencing mussel (*Mytilus trossulus, M. edulis*) settlement on a wave-exposed rocky shore. Mar. Ecol. Prog. Ser. **142:** 135–145.

JONES, W. E., AND A. DEMETROPOULOS. 1968. Exposure to wave action: Measurement of an important ecological parameter on rocky shores of Anglesey. J. Exp. Mar. Biol. Ecol. **2:** 46–63.

KOBAYASHI, N. 1999. Numerical modelling of wave runup on coastal structures and beaches. Mar. Tech. Soc. J. **33:** 33–37.

———, AND Z. DEMERBILEK [EDS.]. 1995. Wave forces on inclined and vertical structures. American Society of Civil Engineers.

KOEHL, M. A. R. 1977. Effects of sea anemones on the flow forces they encounter. J. Exp. Biol. **69:** 87–105.

———. 1979. Stiffness or extensibility of intertidal algae: A comparative study of modes of withstanding wave action. J. Biomech. **12:** 634–646.

———. 1996. When does morphology matter? Annu. Rev. Ecol. Syst. **27:** 501–542.

LEVIN, S. A., AND R. T. PAINE. 1974. Disturbance, patch formation, and community structure. Proc. Natl. Acad. Sci. USA **71:** 2744–2747.

MENGE, B. A. 1976. Organization of the New England rocky intertidal community: Role of predation, competition, and environmental heterogeneity. Ecol. Monogr. **46:** 355–393.

PAINE, R. T. 1966. Food web complexity and species diversity. Am. Nat. **100:** 368–378.

———. 1979. Disaster, catastrophe, and local persistence of the sea palm *Postelsia palmaeformis.* Science **205:** 685–687.

———, AND S. A. LEVIN. 1981. Intertidal landscapes: Disturbance and the dynamics of pattern. Ecol. Monogr. **51:** 145–178.

SARPKAYA, T., AND M. ISAACSON. 1981. Mechanics of wave forces on offshore structures. Van Nostrand-Reinhold.

SOUSA, W. P. 1984. Intertidal mosaics: Patch size, propagule availability, and spatially variable patterns of succession. Ecology **65:** 1918–1935.

THORNTON, E. B., AND R. T. GUZA. 1983. Transformation of wave height distributions. Journal of Geophysical Research **88(C10):** 5925–5938.

TRENBERTH, K. E. 1993. Northern hemisphere climate change: Physical processes and observed changes, p. 35–39. *In* H. A. Mooney, E. R. Fuentes, and B. I. Kronberg [eds.], Earth systems responses to global changes: Contrasts between North and South America. Academic Press.

VOGEL, S. A. 1994. Life in moving fluids, 2nd ed. Princeton Univ. Press.

WELLINGTON, G. M., AND R. B. DUNBAR. 1995. Stable isotope signature of El Niño–Southern Oscillation events in eastern topical Pacific reef corals. Coral Reefs **14:** 5–25.

WETHEY, D. S. 1985. Catastrophe, extinction, and species diversity: A rocky intertidal example. Ecology **66:** 445–456.

Received: 14 June 2002
Accepted: 12 December 2002
Amended: 30 December 2002